RBRH

Revista Brasileira de Recursos Hídricos
Brazilian Journal of Water Resources
Versão On-line ISSN 2318-0331
RBRH, Porto Alegre, v. 23, e1, 2018
Scientific/Technical Article

http://dx.doi.org/10.1590/2318-0331.0318170023

Characterization of the Capibaribe River Dry Bed with Ground Penetrating Radar (GPR)

Caracterização do Leito Seco do Rio Capibaribe com o Radar de Penetração do Solo (GPR)

Gracieli Louise Monteiro Brito[1], Artur Paiva Coutinho[2,3], Jaime Joaquim da Silva Pereira Cabral[2,3], Severino Martins dos Santos Neto[2,3], Antonio Celso Dantas Antonino[2,3], José Almir Cirilo[2,3], Ricardo Augusto Pessoa Braga[4] and Severino Lopes da Silva Filho[2,3]

[1]Instituto Federal de Educação, Patos, PB, Brazil
[2]Universidade Federal de Pernambuco, Caruaru, PE, Brazil
[3]Universidade Federal de Pernambuco, Recife, PE, Brazil
[4]Águas do Nordeste, Recife, PE, Brazil

E-mails: gracielimonteiro@yahoo.com.br (GLMB), artur.coutinho@yahoo.com.br (APC), jcabral.ufpe@gmail.com (JJSPC), martins.dsn@gmail.com (SMSN), acdantonino@gmail.com (ACDA), almir.cirilo@gmail.com (JAC), rbraga@hotlink.com.br (RAPB), slsfilho@yahoo.com.br (SLF)

Received: February 08, 2017 - Revised: July 04, 2017 - Accepted: August 06, 2017

ABSTRACT

For an adequate hydrogeological study of alluvial layers in the semi-arid zone, it is important to know well its geometry and its hydraulics characteristics. Alluvial formations are generally constituted by erosion, transport and sedimentation processes, causing considerable heterogeneity in soil hydraulic parameters and water flow. The present research had as objective to perform a geophysical characterization using the Ground Penetrating Radar – GPR in the dry bed of the Capibaribe river. To the extent that depositional layers exhibit changes in water content, granularity, sediment type and layer orientation, the water table as well as sedimentary structures and lithological contacts tend to be identified, making the method effective for hydrogeology research. The study area comprises alluvial dry river bed of upper Capibaribe river in the municipality of Santa Cruz do Capibaribe. The results showed that GPR was efficient in the imaging of the subsurface contributing to the knowledge of the geometry and the stratigraphy of the aquifer of the dry bed of the river. In the dry bed of the river, with 400 MHz antenna the signal reached a depth of 2.65 m, and with the antenna of 200 MHz, the signal reached a depth of 6.00 m. The capillary fringe was identified at a depth of 3.0m with the use of 200MHz and 400MHz antennas.

Keywords: GPR; Alluvium; Semiarid.

RESUMO

Para um estudo hidrogeológico adequado de camadas de aluvião no semiárido é importante conhecer bem sua geometria e suas propriedades. As formações aluviais são geralmente constituídas por processos de erosão, transporte e sedimentação, causando considerável heterogeneidade nos parâmetros hidráulicos do solo e no fluxo de água. A presente pesquisa teve como objetivo realizar uma caracterização geofísica através do Radar de Penetração no Solo – GPR no leito seco do rio Capibaribe. As mudanças nas camadas no conteúdo de água, granulometria, tipo de sedimento e orientação das camadas, o lençol freático, as estruturas sedimentares e os contatos litológicos tendem ser identificados, o que torna o método eficaz para investigação hidrogeológica. A área de estudo compreende as aluviões do leito seco do alto Capibaribe no município de Santa Cruz do Capibaribe. Os resultados mostraram que o GPR foi eficiente no imageamento da subsuperficie contribuindo para o conhecimento da geometria e da estratigrafia do aquífero do leito. No leito seco do rio, com antena de 400 MHz o sinal atingiu profundidade de 2,65 m e com antena de 200 MHz o sinal atingiu 6,00 m. A franja capilar foi identificada na profundidade de 3,0 m com o uso das antenas de 200MHz e 400MHz.

Palavras-chave: GPR; Aluvião; Semiárido.

INTRODUCTION

In the Brazilian semi-arid northeast, the evapotranspiration rates are extremely high. Thus, it is preferable to store water in the subsoil than at the surface when willing to protect the water from the wind and insolation. Thereby, it is possible to achieve a very significant reduction of evaporative losses.

Most of the northeastern semiarid are geologically formed by the crystalline rock very close to the surface (less than 1.00 meter) or even outcropping in some points. The option is to store water in the alluvium layers in the valleys, which accumulate sediments carried by storm waters.

The Ground Penetration Radar (GPR) is a tool with great potential to provide information about the alluvium layers. It enables, in a non-invasively way, the inference of the characteristics of the accumulated sediments, their thickness, the configuration of the rocky base and the existence of fractures and failures.

The radar frequencies in the range of 10 to 1000 MHz are indicated in order to acquire information related to the subsurface, locate structures and geological and shallow pedological features. The reason for this is that the transmitted electromagnetic waves reflect in the soil and rocks layers with different electrical properties, producing an image of the reflectors in the subsurface (ANNAN, 2001). The electrical properties of the soil and/or rock depend on the mineralogical composition and the water content. Thus, reflections of the electromagnetic waves are produced, when the top of the water table or a change in the geological structure is found. Higher frequencies lead to higher spatial resolutions, but also to greater attenuation and, consequently, to a lower penetration depth. Lower frequencies lead to greater depth of penetration and lower information resolution.

GPR can be applied in the resolution of the most diverse problems. It can be used in the engineering, environment, geology or even to solve forensic problems. As a support to hydrogeological studies, the applied geophysics assumes a fundamental role, contributing directly to the understanding of the geological and hydrogeological model in the subsurface (COUTINHO et al., 2015), reducing project costs and execution time.

Lima et al. (2009) applied the GPR to three alluvial deposits in the Brazilian semi-arid region. They verified that the GPR was efficient in imaging the interface between the alluvial sediments and the crystalline rock, generating subsidies for the design of underground dams.

Steelman and Endres (2012), Barbosa et al. (2010), Gacitúa et al. (2012), Schmalholz et al. (2004) and Paixão et al. (2006) applied the GPR to estimate the moisture spatial variation. These studies have been conducted both in the field real conditions and in the laboratory. Several frequencies in the range of 10MHz to 900MHz have been used in these applications. In the work of Steelman and Endres (2012), Gacitúa et al. (2012) and Schmalholz et al. (2004)), the acquisition of speed profiles using the common-midpoint-CMP technique allows the estimation of the spatial variability of the moisture profiles in the field. This is possible because of a physical relationship between the moisture, the propagation speed of the electromagnetic wave, the dielectric constant and soil parameters, such as particle specific mass and porosity. The frequencies of 400 and 900 MHz have been the most used. Steelman and Endres (2012) have demonstrated that the profiles obtained with the 900 MHz antenna allowed a greater precision in the estimation of the humidity.

McClymont et al. (2010), Farmani et al. (2008), Lu and Sato (2007), Loeffler and Bano (2004) used the GPR to obtain information about the water table and subsoil.

Daniels et al. (1995), Benson (1995), Benson et al. (1997), Moreira and Braga (2009), Cavalcanti (2013), Win et al. (2011), Botelho et al. (2003) applied the GPR to identify the contamination caused by hydrocarbons or oils in the groundwater. In these works, the principle of interpretation of contaminated zones is the identification of regions with resistivity contrast. That is, regions with low electrical resistivity result in attenuated zones in the radargrams.

The present article presents a study conducted in a dry stretch of the Capibaribe River, which is located in the upper part of the hydrographic basin. The objective of this study is to evaluate the visualization capacity of the water table and the interface between the sedimentary layer and the rocky top using GPR.

SOIL PENETRATION RADAR – GPR

The sedimentary layer can be considered as composed of a dielectric material, which has magnetic permeability properties, electrical conductivity, and dielectric permittivity, which depend on the sediments composition. They also depend on the size, shape, grain orientation and arrangement, and porosity.

The main cause of GPR reflections in sediments is attributed to changes in the dielectric permittivity, mainly due to the presence of water (NEAL, 2004). Some factors such as the presence of organic matter, the precipitation of iron oxide, besides the granularity distribution of the sediments and the connectivity between the pores, influence the water content.

The presence of the organic matter that exists in distinct horizons in the soils sets important limits within the sedimentary sequence. Another non-sedimentary feature that can be identified in GPR profiles, depending on the dielectric properties contrast, is the reflection of the top of the water table, that generally presents a horizontal or gently sloping surface that cuts primary sedimentary structures. Before collecting the data and during the laboratory processing should be taken into account that there are subsurface features that can generate reflections, but they are not necessarily bound to primary sedimentary structures (NEAL, 2004).

The GPR operation principle is based on the propagation theory of electromagnetic waves, and on the principle of transmission and reflection of these waves. The theoretical foundation is based on Maxwell's equations, which describe the behavior of electric and magnetic fields in macroscopic situations. Maxwell's equations are described by four laws, each representing a generalization of certain experimental observations: i.) Faraday's law (a magnetic field generates an electric field in a closed circuit); ii.) Ampere's Law (an electric current generates a magnetic field); iii) Gauss's law for the electric field and iv.) Gauss's law for the magnetic field (ANNAN, 2001).

The introduction of the medium constitutive relations into Maxwell's equations translates, through physical properties, the interactions between the electromagnetic fields of a given source with a medium. **Electric Conductivity (σ)** - describes

the flow of electric charges produced by an electric field; **Dielectric Permittivity (ε)** - describes how intrinsic loads to the material can be displaced in response to an electric field. In GPR studies are normally used the relative dielectric permittivity, $\varepsilon_r = \varepsilon / \varepsilon_o$, where: ε is the dielectric permittivity of the material (F/m), and ε_o is the vacuum dielectric permittivity $\left(8{,}854x10^{-12} F/m\right)$ (BORGES, 2002); **Magnetic Permeability ($\tilde{\mu}$)** - is defined as the magnetization degree of a material in response to a magnetic field.

Maxwell's equations present fundamental relations to obtain information on the electrical properties of the materials, through which the electric and magnetic fields work. They are: Relation between current density and electric field (Ohm's Law), direct relation to the electric field and the displacement current, relationship between the magnetic field ($\overline{H}$) and the magnetic induction field ($\overline{B}$) (BORGES, 2002).

One of the main limitations of the GPR method is its application in clay medium, or where there are ores with high iron concentration and magnetic iron composition, as well as in high electrical conductivity medium. In these cases, the high energy attenuation of the electromagnetic wave creates difficulties in obtaining good resolution and penetration depth in the soil.

According to Pinto (2010) and Rijo (2004), the penetration depth and the losses associated with the propagation of electromagnetic waves in the geological environment can be measured by the *"skindepth"* parameter (δ). Reynolds (1997) defines this parameter as the penetration depth at which the amplitude of the electromagnetic wave α is reduced to 36.79% of its initial value, see Equation 8. This equation is applied to non-magnetic means, i.e., $\mu = \mu o = 4\pi.10e\text{-}7$ H/m and $\omega = 2\pi f$, with f being the central frequency of the GPR operation. Thus:

$$\delta = \sqrt{\frac{2}{\omega\mu\sigma}} \quad (1)$$

Where: μ is the magnetic permeability, σ is the conductivity in mS/m, ω is the wave pulse or angular frequency. Whereas the ratio $\sigma / \omega\varepsilon < 1$.

In this context, the materials that have a high electrical conductivity present a low penetration depth of the electromagnetic wave. Consequently, materials of low σ values present an increase of the *"skindepth"* parameter, providing a greater penetration.

Antennas types

The antennas can be monostatic when the same antenna is used for signal transmission and reception, or bi-static, when there is an independent antenna for each task, that is, one to transmit and another one to receive the signal. The antenna size determines the characteristics of the transmitted electromagnetic pulse, especially its duration. Thus, a longer pulse requires a larger antenna (COSTA, 2005).

Data acquisition with GPR

The GPR allows the execution of profiles in continuous or discontinuous mode. The continuous mode is performed when the set of antennas (transmitter and receiver) is moved along the survey line, using a mechanism of time or measurement of the covered space as a reference for the emission of the wave. The continuous mode is applied on flat surfaces and without too many obstacles. As for the discontinuous mode, the data are acquired in individual positions. The antennas stay momentarily stationed at each acquisition point during the wave emission. This mode is more suitable for undulating terrain or places with small obstacles (ARANHA, 2010). According to Borges (2007), regarding the acquisition technique, the most used are:

- o Constant Reflection Profiles or "Common Offset": consists of moving a monostatic antenna or two antennas simultaneously on the ground surface. The traces are acquired at a continuous distance or time intervals;
- o Speed surveys: a same point or area is registered redundantly, with different distances. They can be performed by the Wide Angle Reflection (WARR) or Common-midpoint (CMP) technique. In the CMP technique, the aperture between the antennas (transmitter and receiver) increases in opposite directions, starting from a fixed center point. In the WARR technique, one of the antennas is held fixed while the other is successively pulled apart from the first;
- o Transillumination or tomography mode: for structural evaluations, when searching for the identification of the piece integrity through the presence of fissures, voids, reduction of the steel sections constituent of the armature or still used during the drilling of wells and mines (LOPES, 2009). It is used to measure the speed inside bodies or solid objects efficiently. (COSTA, 2005).

According to Borges (2002), besides the CMP / WARR surveys there are two other ways of determining the propagation velocity of the electromagnetic wave in the medium:

a) The propagation speed of electromagnetic waves is practically constant for geological material with an electrical conductivity lower than 100 mS/m. In this case, where the loss is very small, and there is no presence of ferromagnetic material ($\tilde{\mu} = 1$), the speed (ν), the attenuation constant (α em dB/m) and the propagation constant (β) can be calculated by Equations 2, 3 and 4:

$$v = \frac{c}{\sqrt{\varepsilon_r'}} \quad (2)$$

$$\alpha = \frac{\sigma}{2}\sqrt{\frac{\mu}{\varepsilon_r}} \quad (3)$$

$$\beta = \omega\sqrt{\mu\varepsilon_r} \quad (4)$$

Where: *v* is the propagation velocity of the electromagnetic wave; εr´ is the relative dielectric permissiveness, *c* is the light speed in the vacuum (≈ 0,3 m/ns), α is the attenuation constant, σ is the electrical conductivity (mS/m), μ is the magnetic permeability, ω is the wavelength, β is the propagation constant.

In Equation 2, it is observed that the wave velocity depends only on the dielectric permissiveness of the GPR signal propagation medium. In GPR systems, normally the speed remains at an essentially constant level for conductivities less than 100 mS/m and the EM field propagates without dispersion (DAVIS; ANNAN, 1989).

Table 1. Dielectric permittivity, electrical conductivity, mean speed and attenuation values for some typical geological materials. Data obtained using an 100Mhz antenna.

Material	Dielectric Permissiveness - ε̃	Electrical Conductivity – σ (mS/m)	Speed – v (m/ns)	Attenuation - α (dB/m)
Air	1	0	0.3	0
Distilled Water	80	0.01	0.033	0.002
Dry Sand	3 – 5	0.01	0.15	0.01
Saturated Sand	20 – 30	0.1 – 1.0	0.06	0.03 – 0.3
Shale	5 – 15	1 – 100	0.09	1 – 100
Silt	5 – 30	1 – 100	0.07	1 – 100
Clay	3 – 40	2 – 1000	0.06	1 – 300

Source: Davis and Annan (1989).

The variations in the electromagnetic properties of some of the most common geological materials are presented in Table 1.

b) the speed estimation can be obtained through wells geological information. The depth of a reflector is determined, being replaced in Equation 5.

$$v = \frac{2h}{t} \quad (5)$$

Where: *h* is the reflector depth, and *t* is the time the wave took to be emitted, reflected and recorded back.

In both the acquisition of reflection profiles and speed probes, the field parameters to be analyzed are antenna frequency, sampling frequency, temporal window aperture, spatial sampling, the spacing between antennas, profile location and orientation and orientation of the antennas (ANNAN; COSWAY, 1992; PORSANI, 1999).

MATERIAL AND METHODS

Study area

The chosen site was in an area in the upper part of the Capibaribe River Basin, more precisely in the Mr. Paulo Fieza Farm. The site geodesic coordinates are latitude 7° 57' 36, 199" S and longitude 36° 18' 42.697" W (Figures 1 and 2), which is located in the municipality of Santa Cruz do Capibaribe. The criteria used to choose this area were: a) there has been no sand extraction there, b) it has good access to equipment/materials transportation and c) has a relatively flat topography that facilitates the sliding of the equipment on the ground.

The experiment venue was the dry bed that is in the main channel of the Capibaribe River. This bed is characterized as an alluvial deposit, with sandy soils of thick texture, with some fractions of fine gravel. The largest bed consists of a geological profile typical of the crystalline geology. More specifically, the study site is located in the Borborema Province, presenting shallow soil and sound rock at a short depth. Several rock outcrops are also observed isolated or immersed in alluvial deposits.

The climate of the region is semi-arid. Thus, presenting negative water balance and average annual rainfall of about 700 mm. Depending mostly on the Intertropical Convergence Zone - ITCZ meteorological systems, which operate between the months of February and May. In the periods when the ITCZ does not operate, the region is subject to long droughts, which is the case of the semi-arid region. The potential evapotranspiration estimated by Thornthwaite and Mather (1955) in this region was between 1200 and 1500 mm per year.

Alluvial deposits in this region are important water storage reservoirs. They meet the needs of the diffuse populations that have access to water through the use of shallow wells.

Soil identification

A granulometric analysis performed the identification of the soils through the constituent particles. The purpose of this test is to assign some texture properties and also to obtain soil parameters such as retention capacity, permeability, porosity and shape factors.

The procedures to determine the soil granularity were performed in the Soil Physics Laboratory - DEN - UFPE, using the ABNT method (ABNT, 1995). This test allowed the determination of the diameters of the finer particles (clay and silt) by sedimentation and the coarser ones (sand) by screening. The test was divided into three parts: coarse screening for fraction larger than 2.0 mm, fine screening for fraction between 2.0 mm and 0.075 mm and sedimentation test for a fraction less than 0.075 mm.

The different sizes of the soil particle determine their texture. The basic textural fractions are sand (size between 0.05 and 2 mm), silt (size between 0.002 and 0.05 mm) and clay (less than 0.002 mm). From the different portions of sand, silt and clay derive the different textural classes.

Procedures for performing the granular distribution test were based on the following standards: ABNT-NBR-6457 (ABNT, 1986) and ABNT-NBR-7181 (ABNT, 1984).

Soil samples collected in the two chosen study areas for the application of GPR were analyzed in the Soil Physics Laboratory of the Nuclear Energy Department at Federal University of Pernambuco.

Equipments and software of GPR data processing

The GPR used in the research is from the Geophysical Survey Systems brand, Inc. (GSSI), SIR 3000 model with 400 MHz and 200 MHz monostatic shielded antennas, including software for visualization and data processing (RADAN 6.6).

Methodology for using the GPR

The following methodology is suggested by Costa (2005) and aims to facilitate the identification of the steps and the definition of the necessary parameters for the success of a GPR exploration. It is divided into eight stages:

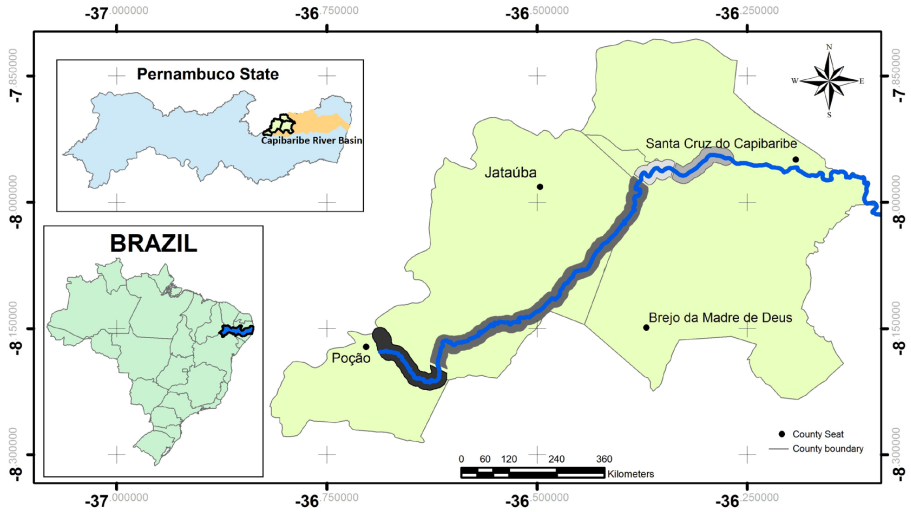

Figure 1. Capibaribe River Basin and location of the study area on the Upper Capibaribe River (PAIVA et al., 2014).

Figure 2. Detailed location of the study area, where area 1 is in the river bed and area 2 in the expanded channel.
Source: Authors' personal files.

1st. Problem definition: The problem type and the desired accuracy degree are going to influence the inherent decisions in the future steps. In general, it is difficult to predict the success of a survey on several geological exploration methods, and the GPR does not escape from this rule.

2nd. Evaluation of the GPR applicability: After defining the problem and its intrinsic difficulties, it should be evaluated if the GPR can be useful for solving the problem. It is possible to find out in advance if the GPR does not produce useful information, so another technique should be used. In general, the GPR is suitable for shallow investigations and for geological materials with high electrical resistivity, whether sandy, rocky or in low humidity conditions. Conductive geological materials, humid and clayey locations, or locations with a considerable percentage of magnetic iron materials are inadvisable for the GPR use.

3rd. Selection of survey method: reflection is the most used method, because it produces an image of the subsoil mapping, being used to locate and identify objects buried underground. In this type of acquisition, the transmitting and receiving antennas are subjected to a constant and fixed distance throughout the acquisition process in the profile. The final result of this acquisition is a two-dimensional radargram with the abscissa axis indicating the distance traveled by the antenna and the ordinates axis representing the round trip time of the electromagnetic signal. The other two methods, CMP or WARR and trans-illumination, are used to

determine the speed propagation of the electromagnetic pulses in the medium.

4th. Definition of the parameters: After having chosen the method, the parameters should be defined, because the correct configuration of parameters leads to more accurate results. Examples of parameters to be configured are the operating frequency of the antennas, the time window between the emitted pulses, the sampling interval of the reflected pulses, the spacing between collection positions, the separation between the antennas, the coordinates of the collection positions and orientation of the antennas.

5th. Data Collection: The process of collecting radargrams begins with the displacement of the antennas at fixed intervals, according to a previously established coordinate system. At the end all collections of the various positions are "stacked" and one or more images are generated.

6th. Pre-processing of data: After obtaining the data or survey images, the next step would be to treat this captured information in order to highlight the features of interest. This step is called preprocessing, and its goal is to increase the chances of success of the next steps. At this moment, a series of treatments with the objective of improving the quality of the geophysical signal demonstrated in the radargrams are applied. The following treatments are applied to increase the energy of the reflectors that have been attenuated: Normalization at distances, position correction, migration to include the propagation speed of the electromagnetic wave and the dielectric constant, and gain as a function of time.

7th. Data analysis: The considerations based on the previous steps are presented in an attempt to verify the possibility of relating the observed data verified in the field with the signals provided with the GPR images. For data analysis, it is necessary to associate the information obtained by visual inspection and direct measurement in situ with their respective geophysical signals demonstrated in the radargram. Thus, it is necessary to relate the real sediment thicknesses, the depth of well-defined targets, the correct depth of the water table and the rocky base with the respective reflectors.

8th. The conclusion of the survey: Finally, based on the analyzed data, a conclusion about what been mapped by the GPR can be made, identifying the expected characteristics, such as geological contacts, faults, rocky top, water depth, and other pedological and hydrogeological characteristics.

GPR Acquisitions in the study area

The GPR data acquisition method used in this research was the technique with constant offset or "common offset". Monostatic antennas with a frequency of 100MHz, 200MHz and 400MHz were continuously used. That is, the set of antennas (transmitter and receiver) was moved along the survey line. Besides that, every 1-meter markings were made.

In July 2014, when the data acquisitions were made, the rainy season has finished in the region and the river was dry. The presence of water in the soil can greatly attenuate the signal of the electromagnetic wave because it increases the value of the electrical conductivity. Thus, the data were acquired after a drought of 5 days in order to avoid possible problems, and the influence of rainfall moisture on the results to be obtained.

The applications with the GPR were carried out in two areas: 1) in the main bed of the Capibaribe River (Case 1) and 2) in the secondary channel of the River (Case 2). In case 1, with the aid of a backhoe, a trench with a depth of 1.30m was built. Whereas in case 2, a trench with a height of 2.30m was built on the slope.

In case 1, the main bed of the river can be seen in Figure 3A, which shows the backhoe constructing a trench of 1.30m depth. The flags placed at the top of the soil were spaced every 40 cm. Besides that, an iron bar of approximately 0.50 m long was buried crosswise at a depth of 1.30 m. The iron bars (Figure 3B) allow the

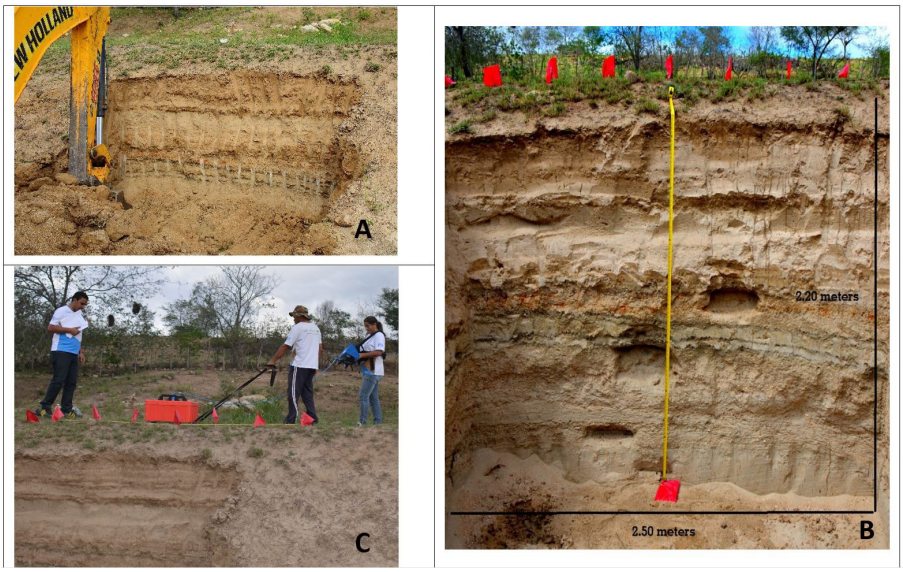

Figure 3. Main bed of the Upper Capibaribe River, application of the 400MHz antenna (Case 1): (A) Construction of the trench; (B) Position of flags and the iron bar and (C) Application with the 400Mhz antenna.
Source: Authors' personal files.

identification of hyperbolic reflectors in the radargram. Therefore, it is possible to estimate the propagation speed of the electromagnetic wave. This technique, aside from helping to calibrate the depth of the reflectors seen in the radargram, also allows the adjustment of the dielectric constant considered in the field.

Figure 3C depicts the acquisitions with a 400 MHz antenna. A 200Mhz antenna has also been used but the results were not satisfactory, since the vertical resolution was not enough to identify the expected hyperbole in the register. Consequently, the propagation velocity of the wave could not be estimated with the use of this antenna.

In Case 2, secondary channel, a trench with a depth of 2.30 m was constructed (Figure 4A). The flags were placed on top of the ground with a spacing of 50 cm between them, and an iron bar was used at the bottom of the trench (Figure 4B). The acquisitions were performed with antennas of 400MHz and 200MHz parallel to the cut made on the slope (Figure 4C).

Steps for basic data processing

A simplified flowchart adopted in this research is presented in Figure 5. Before starting the image processing, the direction of files that didn´t have the same acquisition sense was reversed using the Reverse File option. The first treatment used was the so-called "Distance normalization". This treatment corrects the fact that the equipment conduction speed in the field is not constant. Thus, treatment is required to equalize the speed, allowing the generation of a horizontal scale, assuming that a constant speed of conduction of the equipment has been used in the acquisition.

After the distance normalization have been performed, the "Position Correction" treatment was executed. This treatment suppresses a portion of the radargram corresponding to the air layer between the GPR and the ground. During the acquisition, the GPR is not perfectly attached to the ground. Thus, the radargrams may present a small horizontal layer relative to the air between the antenna and the ground surface. This layer is not important for the interpretation of the images. Therefore, it should be suppressed.

In the migration, the propagation speed of the electromagnetic wave is informed, making possible to relate the depth to the round trip time of the electromagnetic signal.

The Gain procedure is applied to increase the energy of the attenuated reflectors, usually at the deepest depths.

Data interpretation

In this context, the interpretations used in this research were based on the radargrams reflection configurations, according to the lithology and sediment stratigraphies suggested by Beres and Haeni (1991).

RESULTS AND DISCUSSION

Soil identification

The entire samples set of the sidewall of both excavations are shown in a triangular sand/silt/clay diagram based on United States (1967), Figure 6, with a total of 13 samples.

Figure 4. Secondary trench in the Upper Capibaribe River, Case 2. (A) Construction of the trench; (B) Position of flags and the iron bar and (C) Application with antennas of 400MHz e and 200MHz parallel to the cut made on the slope antenna.
Source: Authors' personal files.

- Inform the file entry and exit directories
- Importation of field data
- Data edition
- Distance normalization
- Position Correction (zero-time)
- Migration
- Time Gain

Figure 5. Simplified flowchart of the processing.

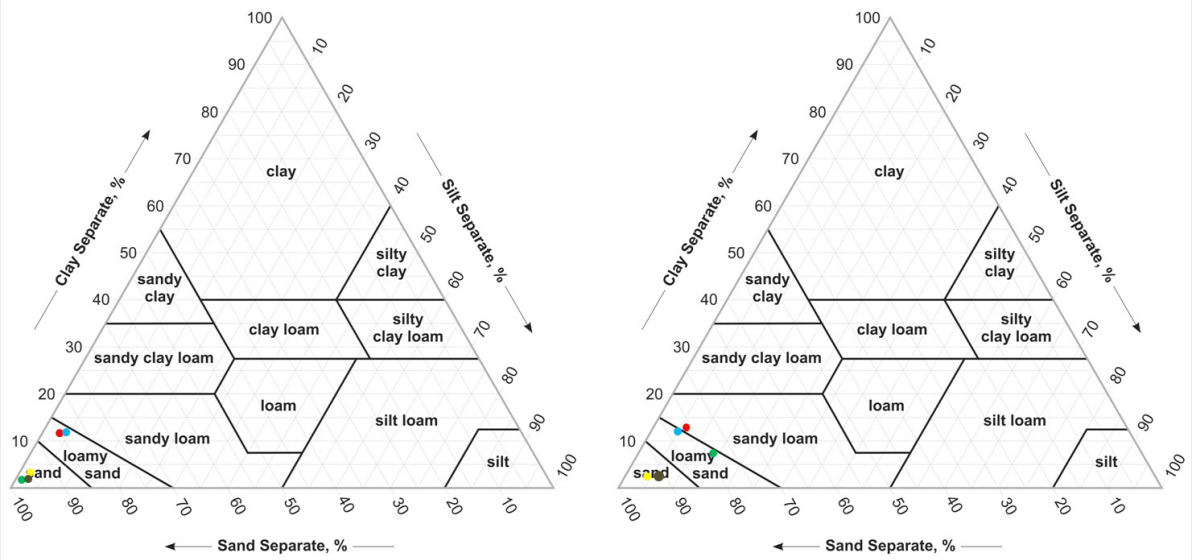

Figure 6. Classification of layers and particle size distribution curve for area 1.

It is verified that the sediment classifications are similar since the granular fractions of sand/silt/clay show little variability. That is, it was checked in the two areas that the percentages of sand are higher than 70%. Besides that, it is noted that the granulometric curves have similar formats for the studied depths. This indicates then that from the granular point of view, there is a certain textural homogeneity of the alluvium between 30 cm and 90 cm for the trench 1. Thus, it is expected a uniformity of dielectric properties, resulting in a signal of same nature between 30 cm and 90 cm.

Interpretation of the GPR images

It is known that each soil produces different signatures on the radargrams. This particularity allied with the penetration depth of the GPR enables the construction of a stratigraphic pattern that characterizes the different features, allowing the differentiation of the soil units (COUTINHO et al., 2015). Thus, based on the literature, some radarfacies with similar characteristics as the one used in this work were individualized in order to facilitate the reading and interpretation of the radargrams, as can be seen in Table 2. These radarfacies can be associated to a distinct lithological set.

The mentioned information applies to the radargrams of Figures 7, 8, 9, 10.

Area 1 – capibaribe riverbed

The radargram obtained with the 400MHz antenna is shown in Figure 7, where it is noted that the signal reached a depth of 2.65 m. Between the depths of 0.40 m to 0.70 m there is a slight attenuation of the signal, which may have been caused by the presence of organic matter. Between the depths of 0.70 m to 1.40 m it is observed that a large part of the record is strongly attenuated. This occurs in function of the variation of the electrical conductivity and is composed of a shadow zone (without reflection), which can be characterized as a region of uniform structure, such as a sand deposit with humidity, which causes little or no dielectric contrast. The propagation velocity was v = 0.1067 m/ns, which was calibrated from the hyperbola generated by the inclusion of an iron bar at a depth of 1.30 m. For the 1.70 m depth, signal attenuation occurs with the presence of a continuous and sub-horizontal reflector, interpreted as a more compacted layer of soil. This region corresponds to zones of high conductivity presenting strong reflections with the presence of sand deposits, as their appearances increase simultaneously with the depth. It is known that in deeper areas less signal or less energy arrives, having then no reflection or diffraction. This leads to the appearance of very conductive areas in the same color as the deeper zones. It was not possible to identify the water table due to the low signal range. However, the water level measured in the two wells, one upstream and one downstream of the analyzed region, were 3.50 m and 2.80 m respectively.

The radargram with the 200 Mhz antenna is shown in Figure 8. The depth reached by the signal was 6.0 m. The iron bar is at a 1.0 m depth, so the calibration of the hyperbola occurred for a wave propagation speed of v = 0.12 m / ns. It is observed that the reflectors are parallel or sub-parallel up to 0.50 m depth, which represents the presence of organic matter and sand. Between 0.50 m and 2.0 m they predominantly present curved and short reflections. In these locations there is a decrease in electrical resistivity, an example are the coarse sand (GOUTALAND et al., 2007). Below the 2.0 m the reflectors are horizontal or sub-horizontal and slightly sloping, continuous and parallel with high amplitude points, that can be related to the existence of fine sand particles with high water content.

Area 2 – secondary channel of the capibaribe riverbed

The radargram obtained with the application of the 400 Mhz antenna in area 2 is shown in Figure 9, where it can be verified that the distance reached by the signal achieved a depth of 5.50 m.

Table 2. Summary of the main radarfacies patterns taken from the GPR sections used in the research.

Radarfacies	Representation	Geometry
Radarfacies A		
Radarfacies B		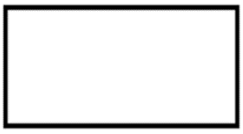
Radarfacies C	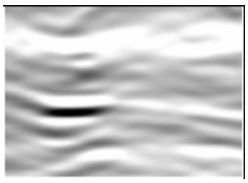	
Radarfacies D	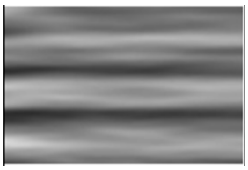	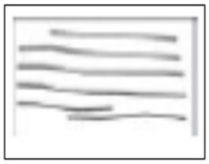
Radarfacies E	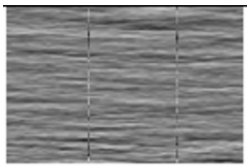	

Where: A - They generally represent horizontal, parallel and continuous reflectors. As well as the presence of organic matter and sand. They are highlighted in red on the radargram; B - They represent strong energy attenuation. Homogeneous soil with a uniform structure, being characterized as a wet sand deposit. They are highlighted in yellow on the radargram; C - They represent oblique reflectors, which can be short and curved. It can be characterized as medium to coarse sand with the presence of moisture. They are highlighted in blue in the radargram; D - They represent horizontal or sub-horizontal reflectors, which are parallel, continuous, slightly inclined. It can be characterized as fine-grained sand with the presence of water. They are highlighted in green in the radargram; E - They represent short and less intense reflectors. It can be characterized as high humidity sand. They are featured in pink on the radargram.

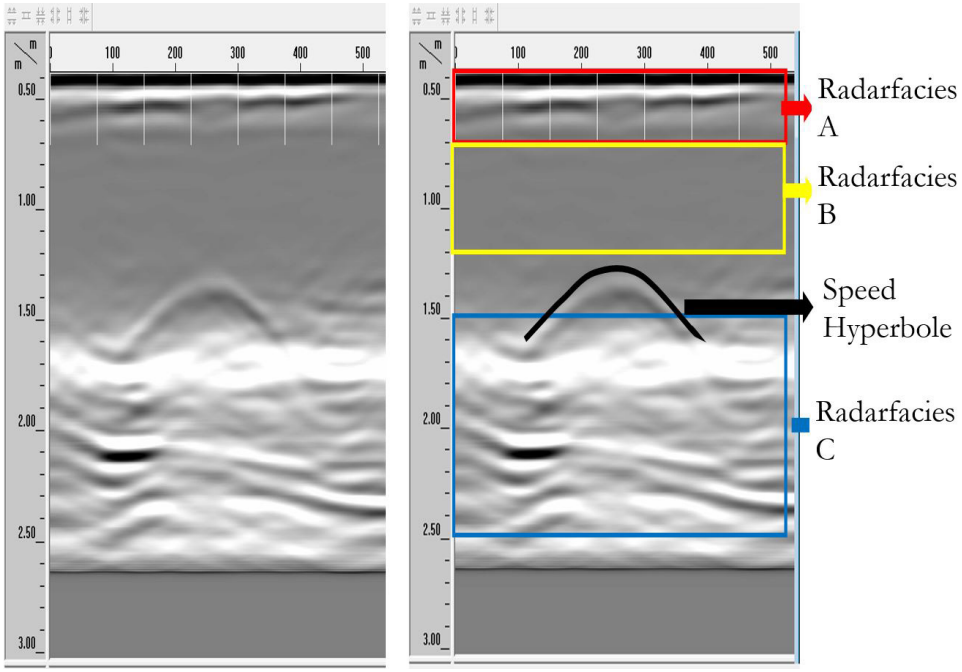

Figure 7. Radargram obtained with the antenna of 400Mhz in area 1 in the main bed of the Capibaribe River (A, B, C are radarfacies, see explanation in Table 2).

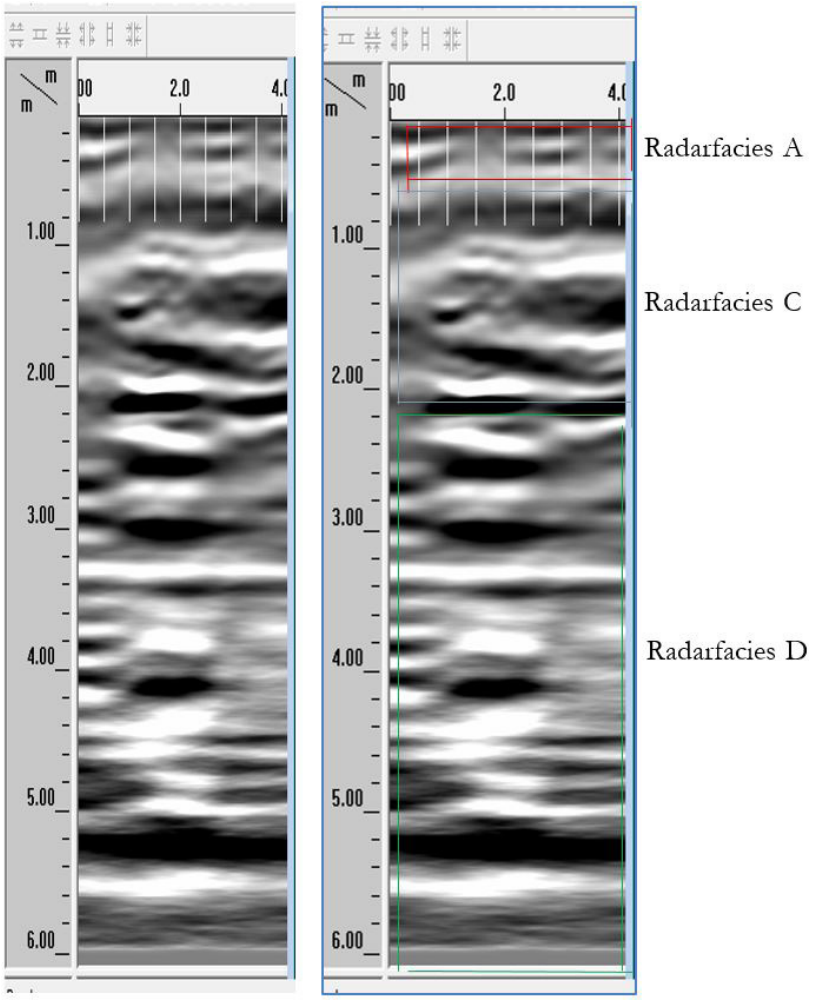

Figure 8. Radargram obtained with the 200 MHz antenna in area 1, in the main bed of the Capibaribe River (A, C, D are radarfacies, see explanation in Table 2).

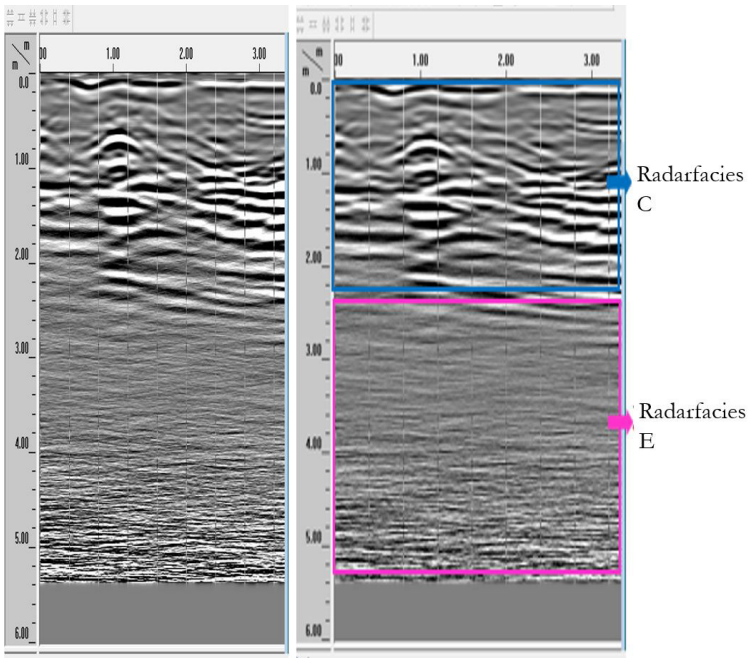

Figure 9. Radargram with the 400 MHz antenna in Area 2, in the secondary channel of Capibaribe River (C and E are radarfacies, see explanation in Table 2).

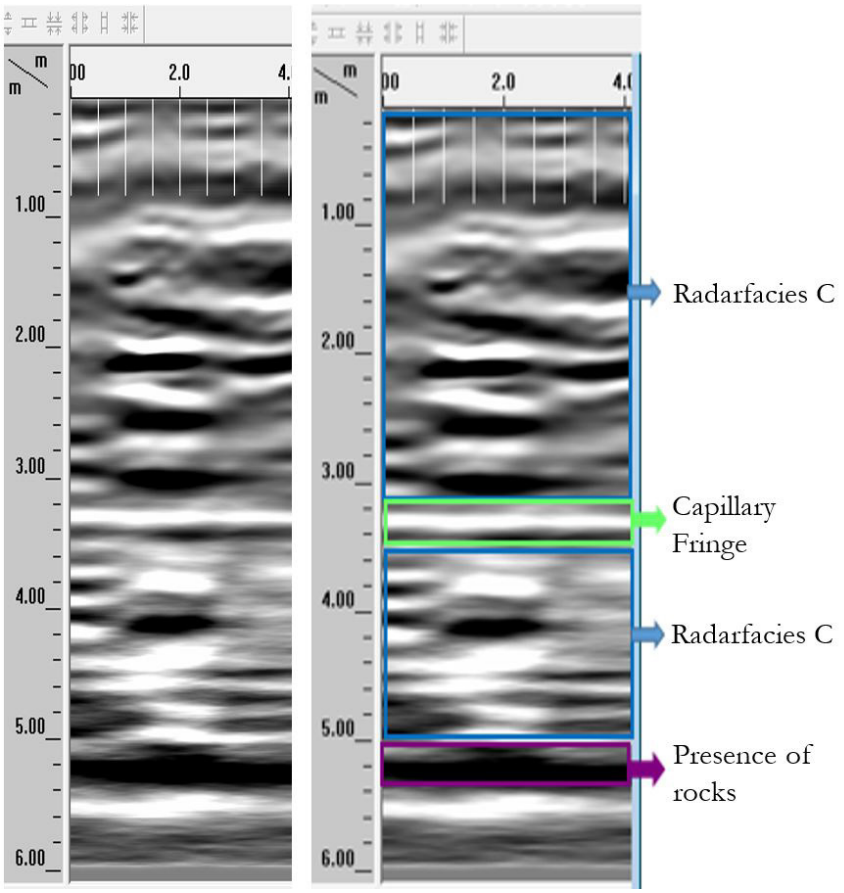

Figure 10. Radargram obtained with the 200MHz antenna in Area 2, in the secondary channel of the Capibaribe River (C are radarfacies, see explanation in Table 2).

Up to a 2.30 m depth, the reflectors obtained in the section present reflections in the form of continuous, horizontal and slightly inclined waves, which are typical of sand (Radarfacies C). In this section C appears in some points hyperbolic features, which may be associated with the presence of boulders. Between 2.30 and 4.0 m, a dispersion of the signal is verified, and it is concluded that there is the presence of radarfacies with chaotic pattern (ANDRADE, 2005). These may be related to the influence of the water table, characterizing the E radarfacies. It is known that the sandy layers are determined from the identification of a weak or small presence of reflectors and an attenuation of the signal (COUTINHO, 2015). Thus, this fact can be verified from over 4.0 m, because zones of signal attenuation take place, which may be characterized by the presence of less intense reflectors.

The radargram obtained with the 200Mhz antenna is shown in Figure 10. It can be seen that the radarfacies presented are continuous, corrugated, parallel and horizontal. They are mostly characterized by radarfacies C, which refers to medium to coarse sand with presence of moisture. At a depth of 3.10 m there is a strong continuous and horizontal reflection, with a high dielectric contrast that can be understood as being a region of higher humidity. This signal attenuation may indicate the presence of the capillary fringe. The margin is high because of the sandy soil and the capillary fringe. Thus, the finer is the medium granulation, the greater will be the thickness reached by the capillary fringe above the water table. This happens due to the capillary suction effects. Below 5.0 m occur regions with low amplitude, dark regions, suggesting the presence of a structure such as rocks. The rocky outcropping near the analyzed region is shown in Figure 11.

Comparison between radargrams obtained with dry soil × wet soil

The comparison of the radargrams obtained with the 400 MHz antenna in two different campaigns in area 2 is shown in Figure 12. It can be noted that the penetration depths diverge as a function of different dielectric properties resulting from the difference of humidity in the sediments, which is caused by rainfall. Probably, the increase of moisture has intensified the energy attenuation of the electromagnetic wave, resulting in differences in depth. For this reason, it is essential to analyze the total amount of precipitated water in the days before the equipment application. The rainfall monitoring for this analysis was obtained from a rain station installed close to the GPR application site. The precipitation variation in the analyzed period in the 1st field campaign, which occurred on July 2, 2014, is shown in Figure 13. At the time, the total precipitated in the previous five days was 5.5 mm and in the second survey campaign, which was on July 29, 2014, was 13 mm.

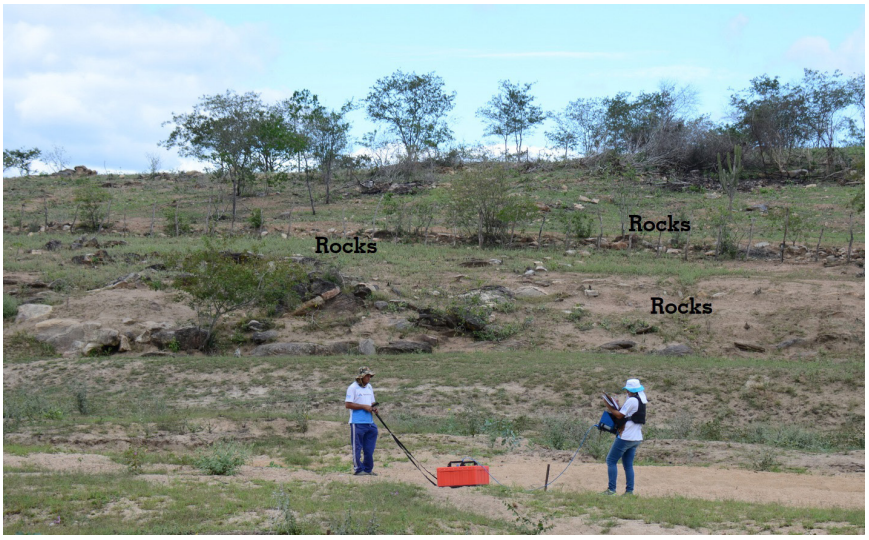

Figure 11. There are rocky outcrops in the surroundings of the GPR application.

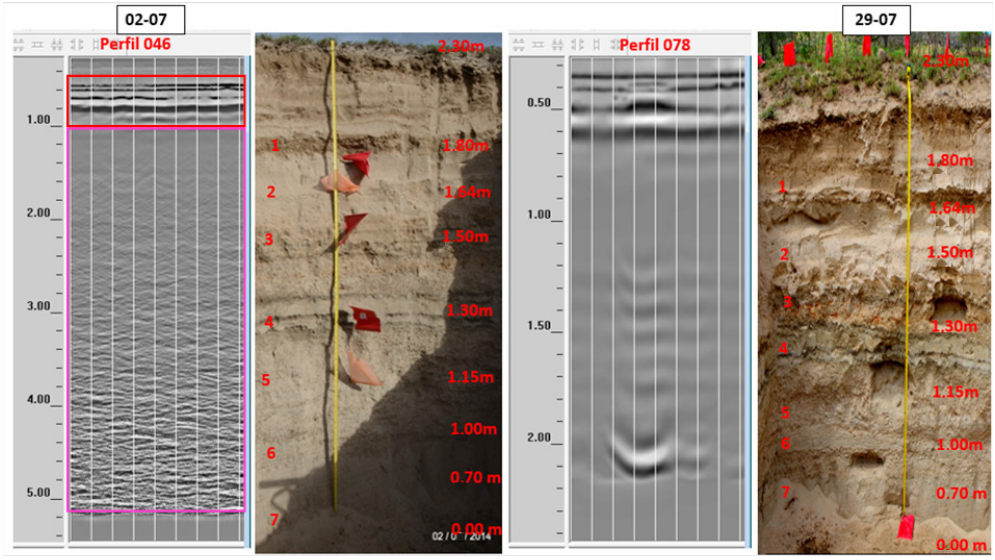

Figure 12. Comparison between radargrams obtained on July 02, 2014 and July 29, 2014.

However, it rained 6.5 mm a day before the experiment performance. Considering this fact, it can be observed that the radargram of the campaign of July 02 presented more details with more reflectors and a higher penetration of the electromagnetic wave when the soil profile was drier. Nonetheless, in the radargram of July 29, although it is wetter than on July 02, it is possible to identify the different layers, because of the low penetration reached by the wave. It is concluded that the soil moisture conditions interfere with the interpretation of the images. The iron bar could not be viewed on the profile 46 (Figure 12) because of the scale that is shown in the radargram. In profile 46, up to the approximate depth of 0.95 m, the feature is characterized by parallel and horizontal reflectors, which are characteristic of organic matter or compacted material layers, classified as A radarfacies. After this range, the profile approaches the type E radarfacies. Bellow the 3.0 m depth it is observed a material with a distribution of parallel segments in small wedges. That is small depositions that are geometrically organized and typical of alluvium sediments.

The radargrams obtained with the 200 Mhz antenna on July 02, 2014 and July 29, 2014, are shown in Figures 14 and 15, respectively. In the radargram of July 02, 2014, up to 2.80 m parallel and rectilinear reflectors are identified, which may characterize the presence of the capillary fringe. The water level of two wells near the application area was measured. For the upstream well the level was 3.50 m and for the downstream well was 2.80 m, where the distance between them approximately 800 m. In the depths around 5.80 m – 6.0 m the reflection that appears can be identified as the rocky top.

As can be noticed, the distances traveled by the signal are different in the two applications. The first campaign (Figure 14)

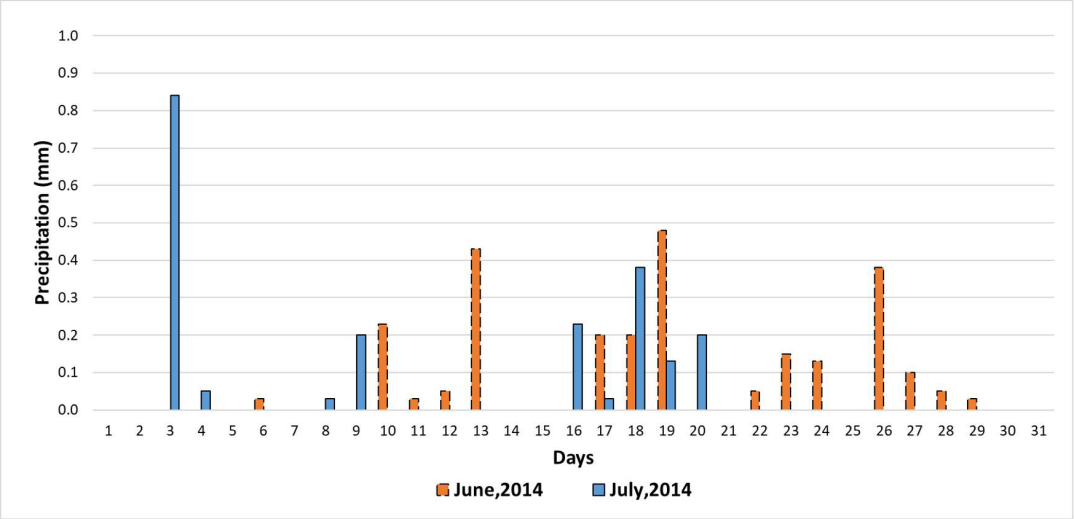

Figure 13. Daily precipitation on June and July 2014 near GPR experimental site.

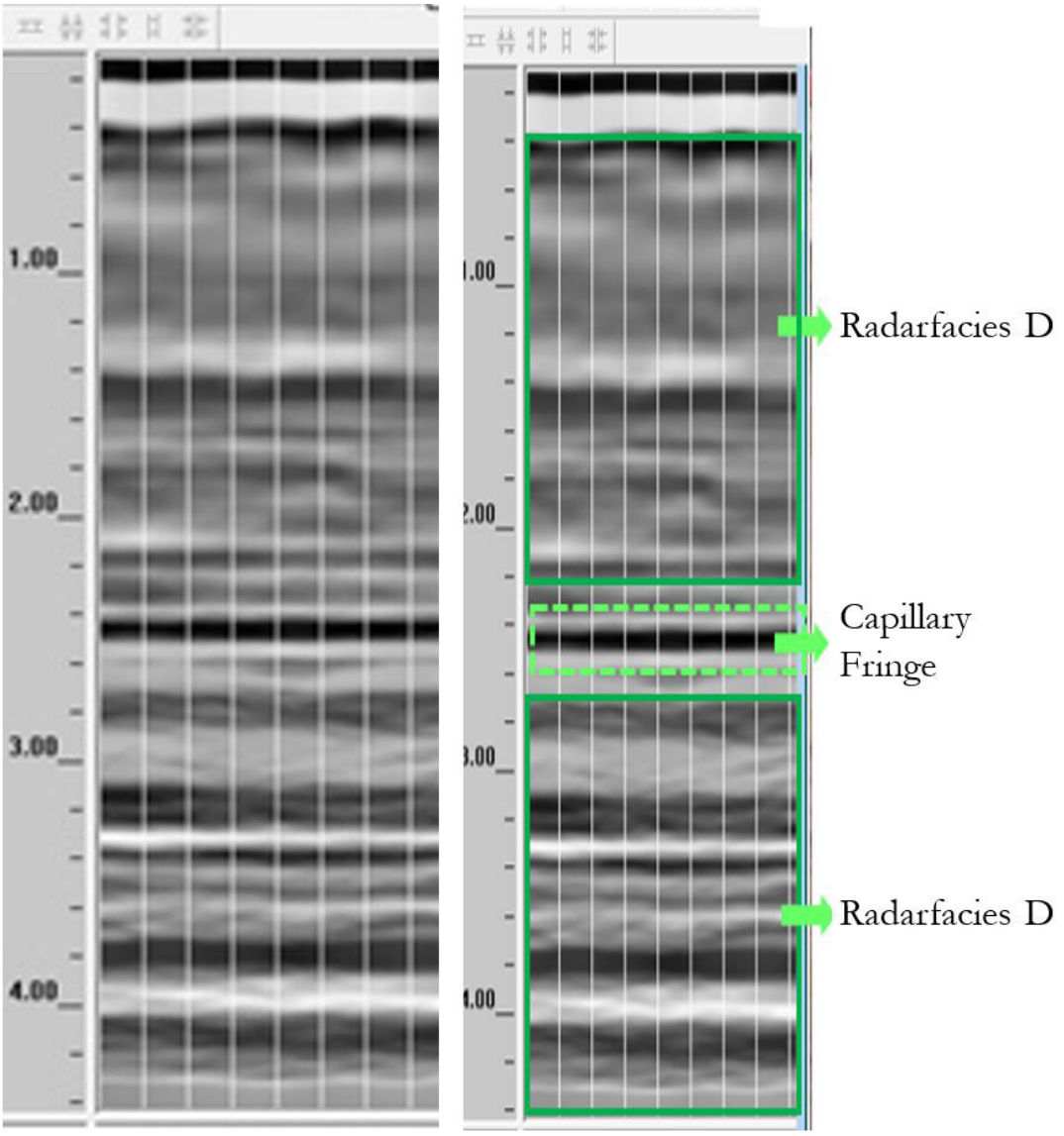

Figure 14. Radargram obtained with the 200 MHz antenna in July 02, 2014 (D is a kind of radarfacies, see explanation in Table 2).

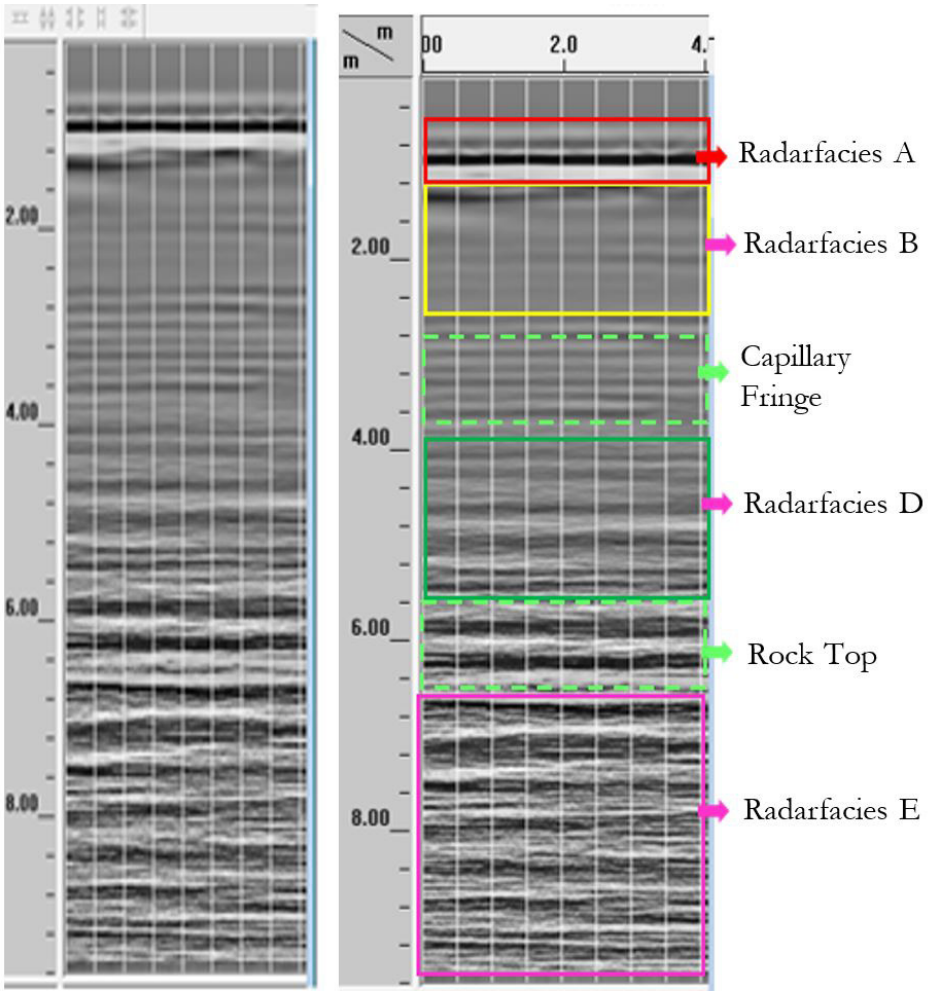

Figure 15. Radargram obtained with the 200 MHz antenna in area 2 on July 29, 2014 (A, B, D, E are radarfacies, see explanation in Table 2).

reaches the depth of 9.0 m and the second (Figure 15), reaches 4.5 m. In this second acquisition, it is possible to observe that in spite of the low penetration, there is a correspondence of the radargram with the horizontal layers of the soil profile. Due to the wetter site, an elevation of the capillary band to 2.50 m can be identified. The attenuations that appear in the depths of 3.30 m and 4.0 m can be interpreted as features correlated to the stratifications.

FINAL CONSIDERATIONS

The annual rainfall in the northeastern semi-arid is not very small, but evaporation losses are very high. Besides that, the soil, with almost outcropping crystalline basement, provides few storage possibilities. A possibility of water storage exists in the alluvial of intermittent dry river beds. There the water accumulates in the pores of the sandbed, and the sand layer protects the groundwater from direct insolation and wind speed, reducing or avoiding losses through evaporation. The stored volumes can be optimized with techniques that improve infiltration capacity and by underground dams that prevent accumulated water from being lost by downstream percolation. Further, the storage capacity and protection against evaporation can be reduced or destroyed if the sand layer is removed to be used in the construction industry, as has been occurring in some places in Pernambuco and Paraiba.

The granulometry tests showed that there is vertical heterogeneity, with some layers of fine sand and others of coarser sand. Even in some depths, larger grains could be found, which can be characterized as gravel.

This fact indicates that in previous times rains were much more intense. Consequently, the velocities and flows of the river were much larger in the past, presenting great capacity of sediment erosion and transportation.

Using the GPR (Ground Penetration Radar), with the 200MHz and 400Mhz antennas, was possible to verify in the two areas the presence of the capillary fringe at a depth of around 3.0 m. This was identified as an attenuation zone of the electromagnetic signal. In area 2, the presence of a dark reflector could also be observed, which refers to the presence of some rocks at 5.0 m depth, in this locality.

The identification of the lithofacies, the rocky top, and the water table could be done through the interpretations of the radargrams. Should be highlighted that most of the radarfacies

found in the riverbed region are characterized as sand, with variations in the granulometry and humidity. The low depth range obtained with the GPR method is sometimes associated with the presence of water. For example, according to the literature, in the application of a 200MHz antenna, a depth of 9.0 meters can be reached (GSSI, 2013). But, in the present study for area 2, the radargram presented a depth of 4.5 meters.

The applications of GPR have shown that its use is not trivial and special care for calibration is needed. This can be done using two antennas or, alternatively, excavating at some location to calibrate the responses obtained in the radargram with the material found underground (in the present research the second method was used).

Once properly calibrated, GPR is a powerful tool and allows the rapid survey of a large area. It leads to the acquisition of relevant information about the sediments heterogeneity, the rocky top and the positioning of the water table.

ACKNOWLEDGEMENTS

The authors acknowledge the support of FACEPE for the Ph.D. scholarship of the first author. As well as to the CISA - International Cooperation for the Semiarid project, financially supported by FINEP. And for the reviewers for their significant contributions.

REFERENCES

ABNT – ASSOCIAÇÃO BRASILEIRA DE NORMAS TÉCNICAS. *NBR 6457*: solo - amostras de solo - preparação para ensaios de compactação e ensaios de caracterização. Rio de Janeiro, 1986.

ABNT – ASSOCIAÇÃO BRASILEIRA DE NORMAS TÉCNICAS. *NBR 6502*: rochas e solos - terminologia. Rio de Janeiro, 1995.

ABNT – ASSOCIAÇÃO BRASILEIRA DE NORMAS TÉCNICAS. *NBR 7181*: solo - análise granulométrica. Rio de Janeiro, 1984.

ANDRADE, P. R. O. *Interpretação de dados de GPR com base na hierarquização de superfícies limitantes e na adaptação de critérios sismoestratigráficos*. 2005. 67 f. Dissertação (Mestrado em Geofísica) - Universidade Federal do Rio Grande do Norte, Natal, 2005.

ANNAN, A. P. *Ground Penetrating Radar*: workshop notes. Mississauga: Sensors & Software Incorporated, 2001.

ANNAN, A. P.; COSWAY, S. W. Ground Penetrating Radar survey design. In: SYMPOSIUM ON THE APPLICATION OF GEOPHYSICS TO ENGINEERING, 26-29 April 1992, Oak Brook. *Proceedings*… Illinois: SAGEEP, 1992. p. 329-351.

ARANHA, P. R. A. *Apostila de georadar*. Belo Horizonte: UFMG, 2010. 43 p.

BARBOSA, E. E. M.; PRADO, R. L.; MENDES, R. M.; MARINHO, F. A. M. Estimativas do teor de umidade empregando o método GPR: uma avaliação comparativa em experimentos de laboratório e campo. *Revista Brasileira de Geofísica*, v. 28, n. 4, p. 691-701, 2010. http://dx.doi.org/10.1590/S0102-261X2010000400012.

BENSON, A. K. Applications of ground penetrating radar in assessing some geological hazards: examples of groundwater contamination, faults, cavities. *Journal of Applied Geophysics*, v. 33, n. 1, p. 177-193, 1995. http://dx.doi.org/10.1016/0926-9851(95)90040-3.

BENSON, A. K.; PAYNE, K. L.; STUBBEN, M. A. Mapping groundwater contamination using dc resistivity and VLF geophysical methods – a case study. *Geophysics*, v. 62, n. 1, p. 80-86, 1997. http://dx.doi.org/10.1190/1.1444148.

BERES, M.; HAENI, F. P. Application of Ground Penetration Radar methods in hydrogeologic studies. *Ground Water*, v. 29, n. 3, p. 375-385, 1991. http://dx.doi.org/10.1111/j.1745-6584.1991.tb00528.x.

BORGES, W. R. *Caracterização geofísica de alvos rasos com aplicação no planejamento urbano e meio ambiente: estudo sobre o sítio controlado do IAG/USP*. 2007. 260 f. Tese (Doutorado em Geofísica) - Instituto de Astronomia, Geofísica e Ciências Atmosféricas, Universidade de São Paulo, São Paulo, 2007.

BORGES, W. R. *Investigações geofísicas na borda da bacia sedimentar de São Paulo, utilizando-se GPR e eletrorrestividade*. 2002. 153 f. Dissertação (Mestrado em Geofísica) - Universidade de São Paulo, São Paulo, 2002.

BOTELHO, M. A. B.; MACHADO, S. L.; DOURADO, T. C.; AMPARO, N. Experimentos laboratoriais com GPR (1GHz) em corpos arenosos para analisar a influência da água e de hidrocarbonetos na sua velocidade de propagação. In: VIII CONGRESSO INTERNACIONAL SOCIEDADE BRASILEIRA DE GEOFÍSICA, 8., 14-18 set. 2003, Rio de Janeiro. *Anais*… Rio de Janeiro: SBGf, 2003, 6 p.

CAVALCANTI, M. M. *Aplicação de métodos geoelétricos no delineamento da pluma de contaminação nos limites do aterro controlado do Jokey Clube de Brasília*. 2013. 111 f. Dissertação (Mestrado em Geociências Aplicadas) - Universidade de Brasília, Brasília, 2013.

COSTA, D. Localização e avaliação do estado físico de dutos subterrâneos através de GPR e redes neurais artificiais. Recife: Universidade Federal de Pernambuco, 2005. Trabalho Apresentado na Disciplina de Redes Neurais Individuais.

COUTINHO, A. P. *A importância da heterogeneidade estrutural da zona não - saturada para a modelagem dos processos de transferência de água na meso-escala*. 2015. 160 f. Tese (Doutorado em Engenharia Civil) - Universidade Federal de Pernambuco, Recife, 2015.

COUTINHO, A.; LASSABATERE, L.; WINIARSKI, T.; CABRAL, J.; ANTONINO, A.; ANGULO-JARAMILLO, R. Vadose Zone Heterogeneity Effect on Unsaturated Water Flow Modeling at Meso-Scale. *Journal of Water Resource and Protection*, v. 7, n. 04, p. 353-368, 2015. http://dx.doi.org/10.4236/jwarp.2015.74028.

DANIELS, J. J.; ROBERTS, R.; VENDL, M. Ground penetrating radar for the detection of liquid contaminants. (1995). *Journal of Applied Geophysics*, v. 33, n. 1–3, p. 195-207, 1995. http://dx.doi.org/10.1016/0926-9851(95)90041-1.

DAVIS, J. L.; ANNAN, A. P. Ground Penetrating Radar for High Resolution mapping of soil and rock stratigraphy. *Geophysical Prospecting*, v. 37, n. 5, p. 531-551, 1989. http://dx.doi.org/10.1111/j.1365-2478.1989.tb02221.x.

FARMANI, M. B.; KITTERØD, N.-O.; KEERS, H. Estimation of unsaturated flow parameters using GPR tomography and groundwater table data. *Vadose Zone Journal*, v. 7, n. 4, p. 1239-1252, 2008. http://dx.doi.org/10.2136/vzj2007.0169.

GACITÚA, G.; TAMSTORF, M. P.; KRISTIANSEN, S. M.; URIBE, J. A. Estimations of moisture content in the active layer in an Arcticeco system by using ground-penetrating radar profiling. *Journal of Applied Geophysics*, v. 79, p. 100-106, 2012. http://dx.doi.org/10.1016/j.jappgeo.2011.12.003.

GOUTALAND, D.; WINIARSKI, T.; ANGULO-JARAMILLO, R.; LASSABATÈRE, L.; BIÈVRE, G.; BUONCRISTIANI, J. F.; DUBÉ, J. S.; MESBAH, A.; CAZALETS, H. Hydrogeophysical study of the heterogeneous unsaturated zone of a stormwater infiltration basin. *Bulletin de Liaison des Ponts et Chaussées*, p. 268-269, 2007.

GSSI – GEOPHYSICAL SURVEY SYSTEMS. *Ground penetrating radar explained*. 2013. Available from: <http://www.geophysical.com/whatisgpr.htm>. Access on: 18 out. 2013.

LIMA, A. O.; SOUZA, A. M.; SABADIA, J. A. B.; CASAS, A.; LIMA FILHO, F. P. Utilização do GPR para locação de barragens subterrâneas no semi-árido brasileiro. In: VII SIMPÓSIO BRASILEIRO DE CAPTAÇÃO E MANEJO DE ÁGUAS DE CHUVA, 7., 2009, Caruaru. *Anais*… Caruaru: ABCMAC, 2009. CD-ROM.

LOEFFLER, O.; BANO, M. Ground Penetrating Radar measurements in a controlled vadose zone: influence of the water content. *Vadose Zone Journal*, v. 3, p. 1082-1092, 2004.

LOPES, O. A. *Uso do GPR (Ground Penetrating Radar) em trechos de pavimentos da cidade universitária da UFRJ*. 2009. 202 f. Dissertação (Mestrado em Engenharia Civil) - Universidade Federal do Rio de Janeiro, Rio de Janeiro, 2009.

LU, Q.; SATO, M. *Quantitative hydrogeological study of an unconfined aquifer by GPR along Tuul River in Ulaanbaatar*. 2007. Available from: <http://www.ied.tsukuba.ac.jp/wordpress/wp-cntent/uploads/pdf_papers/tercbull07s2/t7supple2_3.pdf>. Access in: 02 abr. 2013.

MCCLYMONT, A. F.; HAYASHI, M.; BENTLEY, L. R.; MUIR, D.; ERNST, E. Groundwater flow and storage within an alpine meadow-talus complex. *Hydrol Earth Syst Sci*, v. 14, p. 859-872, 2010.

MOREIRA, C. A.; BRAGA, A. C. O. Aplicação de métodos geofísicos no monitoramento de área contaminada sob atenuação natural. *Engenharia Sanitaria e Ambiental*, v. 14, n. 2, p. 257-264, 2009. http://dx.doi.org/10.1590/S1413-41522009000200013.

NEAL, A. Ground – penetration radar and its use in sedimentology: principles, problems and progress. *Earth-Science Reviews*, v. 66, n. 3-4, p. 261-330, 2004. http://dx.doi.org/10.1016/j.earscirev.2004.01.004.

PAIVA, A. L. R.; CAETANO, T. O.; SILVA, D. J.; CABRAL, J. J. S. P.; BRAGA, R. A. P. Ocorrência e características construtivas de poços escavados em aluvião - trecho alto do Rio Capibaribe - PE. In: XII SIMPÓSIO DE RECURSOS HIDRÍCOS DO NORDESTE, 12., 2014, Natal. *Anais*… Natal: ABRH, 2014.

PAIXÃO, M. S. G.; PRADO, R. L.; DIOGO, L. A. Análise do emprego do GPR para estimar o teor de umidade do solo a partir de um estudo na cidade de São Paulo. *Revista Brasileira de Geofísica*, v. 24, n. 2, p. 189-198, 2006. http://dx.doi.org/10.1590/S0102-261X2006000200003.

PINTO, G.P. *O método GPR aplicado a localização de tubulações utilizadas no abastecimento de água na região urbana do município de Belém - Pará*. 2010. 96 f. Dissertação (Mestrado em Ciências - Área de Concentração: Métodos Eletromagnéticos) - Universidade Federal do Pará, Belém, 2010.

PORSANI, J. L. *GroundPenetrating Radar (GPR): Proposta Metodológica de Emprego em Estudos Geológico-geotécnicos nas Regiões de Rio Claro e Descalvado – SP*. 1999. 145 f. Tese (Doutorado em Geociências e Ciências Exatas) - UNESP, Rio Claro, 1999.

REYNOLDS, J. M. *An introduction to applied and environmental geophysics*. Chichester: John Wiley & Sons, 1997. 795 p.

RIJO, L. *Electrical Geophysics*: 1-D Earth Direct Modeling. Belém: UFPA, 2004. 263 p. Available from: <http://www.cmig.ufpa.br/>. Access in: 03 jul. 2009.

SCHMALHOLZ, J.; STOFFREGEN, H.; KEMNA, A.; YARAMANCI, U. Imaging of water content distributions inside a lysimeter using GPR tomography. *Vadose Zone Journal*, v. 3, n. 4, p. 1106-1115, 2004. http://dx.doi.org/10.2136/vzj2004.1106.

STEELMAN, C. M.; ENDRES, A. L. Assessing vertical soil moisture dynamics using multi-frequency GPR common-mid point soundings. *Journal of Hydrology*, v. 436–437, p. 51-66, 2012. http://dx.doi.org/10.1016/j.jhydrol.2012.02.041.

THORNTHWAITE, C. W.; MATHER, J. R. *The water balance*. New Jersey: Drexel Institute of Technology. 1955. 104 p. (Publications in Climatology).

UNITED STATES. Department of Agriculture. *Soil survey laboratory methods and procedures for collecting soil samples*. Washington: Soil Conservation Service, 1967. 50 p. (Soil Survey Investigation Report, 1).

WIN, Z.; HAMZAH, U.; ISMAIL, M. A.; SAMSUDIN, A. R. Geophysical investigation using resistivity and GPR: A case study of

an oil spill site at SeberangPrai, Penang. *Bulletin of the Geological Society of Malaysia*, n. 57, p. 19-25, 2011.

Authors contributions

Gracieli Louise Monteiro de Brito: Main author, author of doctor thesis that originates this paper.

Artur Paiva Coutinho: Interpretation of GPR images obtained in field work.

Jaime Joaquim da Silva Pereira Cabral: Supervisor of doctor thesis that originates this paper.

Severino Martins dos Santos Neto: Field work with GPR equipment, sediment analysis.

Antonio Celso Dantas Antonino: Interpretation of results, infiltration expert.

José Almir Cirilo: Interpretation of results, semiarid expert.

Ricardo Augusto Pessoa Braga: Manager of experimental site, coordinator of "Water from Sand" project, discussion of results.

Severino Lopes da Silva Filho: Field work with GPR equipment, discussion of results.